ATLAS Internal Note
INDET-NO-???

THERMAL MEASUREMENTS OF A PIXEL BARREL STAVE PROTOTYPE

D. Bintinger, J. Emes, M. G. D. Gilchriese, R. A. Lafever and T. Truong
Lawrence Berkeley National Laboratory

W. Miller
Hytec, Inc

ABSTRACT

Measurements of the thermal performance of a full-length, pixel barrel stave prototype type are presented. The temperature distribution in the prototype stave has been measured with methanol-water and with methanol-water-ice("binary ice") coolants. The binary ice coolant provides lower temperature and a more uniform temperature operation. The temperature of simulated silicon modules is everywhere less than -5°C with the binary ice coolant. The temperature distribution measured in the stave for methanol - water coolant is compared successfully to theoretical and finite-element calculations.

I. INTRODUCTION

The ATLAS pixel detector is comprised of barrel and disk elements. The barrel is composed of staves(or ladders) on which the pixel modules are mounted. In this paper, we present measurements of the thermal properties of a full-length, prototype stave, built to simulate the expected thermal properties of a pixel barrel stave.

II. PROTOTYPE STAVE

An end view of the prototype stave is shown in Fig. 1. The stave was fabricated from aluminum and was about 80 cm long. EPO-TEK H20E Silver Epoxy was used to bond the coolant channel to the base plate. Two different thermal epoxies were was used to bond the aluminum piece simulating the silicon modules to the base plate. Both Dymax 991 and Master Bond EP21AN were used for different measurements as indicated below.

The thermal properties of aluminum are close to those of the materials(carbon-carbon(C-C) and silicon) to be used in the final pixel staves, as shown in Table 1. The dimensions of the prototype stave were chosen to simulate the performance of a C-C stave. However, the coolant channel design is likely to be somewhat different in the final staves and thus it is important to be able to model accurately the coolant-channel wall interface to predict performance in other configurations.

Material	Conductivity (W/(m-°K)
Aluminum	168
Carbon-Carbon	40 transverse, 180 in plane
Silicon	150

Table 1. Comparison of the thermal conductivity of aluminum, carbon-carbon and silicon.

III. METHANOL-WATER RESULTS

Measurements of the thermal performance of the prototype stave were made with a 30-70% methanol-water mix at Lawrence Berkeley National Laboratory(LBNL). The prototype stave was mounted in a cold box cooled by liquid nitrogen boil off. The ambient temperature in the cold box was maintained at about -7.5 °C. The methanol-water mixture was circulated by a pump and the flow measured. The pressure drop across the stave was also measured. The inlet and outlet fluid temperatures were measured in small "mixing

stations" to obtain a precise measurement of the bulk fluid temperatures.

These measurements were made with a Dymax adhesive. In addition, the predictions of the

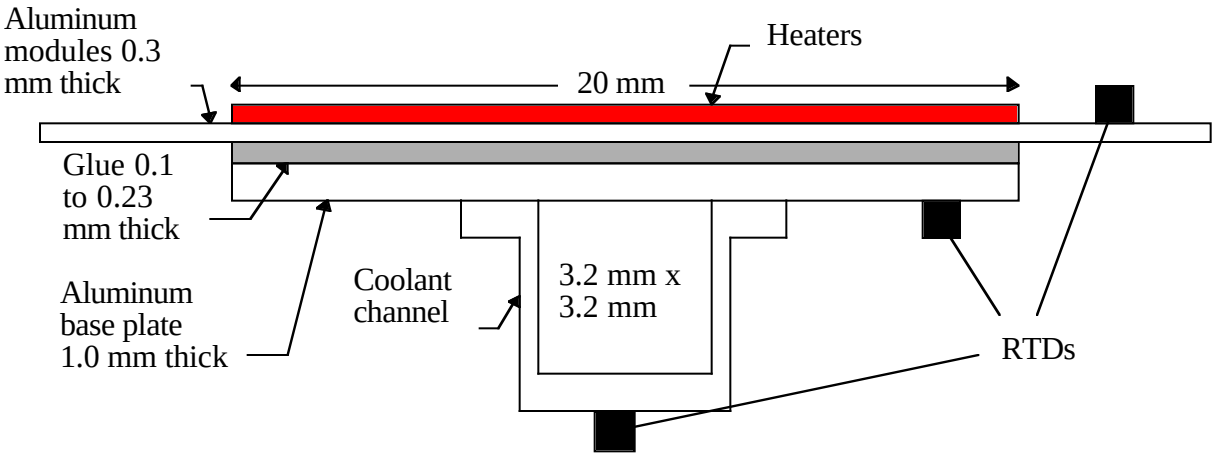

Fig. 1 Cross section view of the prototype stave.

The stave was heated by kapton heaters mounted on top of the "silicon" with a power density of 0.6 W/cm^2 to simulate the expected heat load from the pixel electronics, detector leakage currents and other sources. The temperature distribution in the stave was measured with RTDs mounted on the "silicon", on the coolant base plate and on the bottom of the coolant channel(see Fig. 1). The inlet fluid temperature for these measurements was about -15^{o}C. The temperature measurements along the stave are shown in Figs. 2 - 4 for the "silicon", the base plate and the bottom of the stave, respectively.

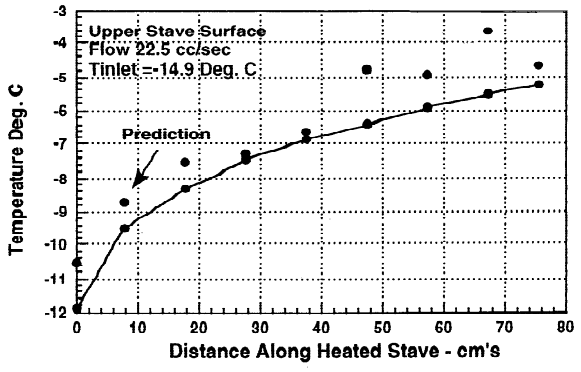

Fig. 2 Temperature distribution of the "silicon" on the prototype stave vs distance along the stave. The solid line shows the predicted behaviour.

temperature distribution (described in the next section) are also given. These measurements were obtained with a fluid flow of 22.5 cm^3/sec. The predictions are in reasonable agreement with the measurements. Some of the discrepancy for the "silicon" temperature(Fig. 2) can be ascribed to poor glue bonding, that was later verifed by inspection.

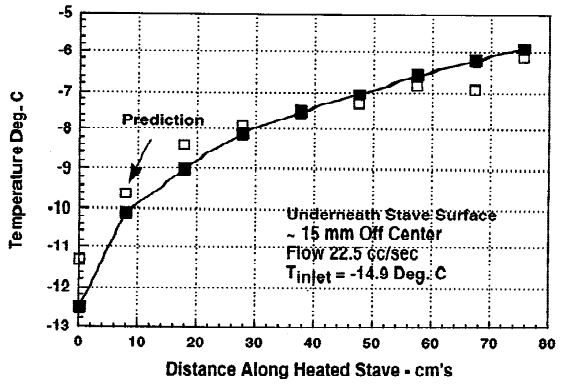

Fig. 3 Temperature distribution of the base plate underneath the "silicon" on the prototype stave vs distance along the stave. The solid line shows the predicted behaviour.

Measurements were also made at a lower flow rate of 13.5 cm^3/sec, which corresponds to a pressure drop of about 200 mbar, the allowed

pressure drop across a stave for leakless operation in ATLAS. The temperature distribution for the base plate for these conditions is shown in Fig. 5.

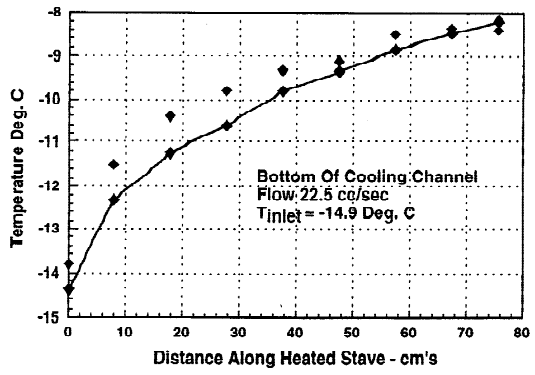

Fig. 4 Temperature distribution of the bottom of the coolant channel on the prototype stave vs distance along the stave. The solid line shows the predicted behaviour.

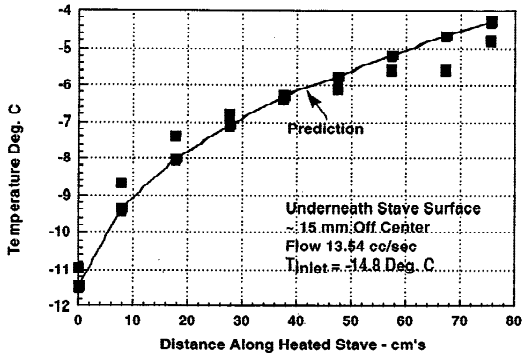

Fig. 5 Temperature distribution of the base plate of the prototype stave vs distance along the stave for a pressure drop of 200 mbar. The solid line shows the predicted behaviour.

IV. THERMAL MODELING

The predicted thermal performance is obtained by a combination of analytical calculation and finite-element simulation at each temperature measurement point on the stave. A thermal gradient exists from the outermost pixel module electronics region (strip heater for test) to the coolant. If one were to discount thermal entry effects, the thermal gradient would be simply two dimensional i.e., simply transverse to the flow direction. However, the cold methanol/water mixture is effectively a high Prandtl number fluid, i.e., the laminar velocity profile is established more quickly than the thermal boundary layer. Heat flow in a laminar flow regime occurs by conduction. The temperature gradient in the fluid at the wall is a function of the fluid thermal conductivity, fluid heat capacity, and mass transport. This effect gives rise to a longitudinal temperature gradient. As the fluid next to the wall enters the heated region, it becomes heated, increasing in temperature as the thin lamina picks up heat. This gradient continues to extend into the fluid until the gradient is fully established. At this point the flow is in thermal equilibrium. This effect adds a third dimension to the heat flow equation. Superimposed over this gradient is a temperature gradient associated with heat conduction through the support structure and adhesives that join the structure together.

The geometry of the fluid containment structure and its material thermal conductivity can affect the longitudinal variation in stave temperature. Structures with high thermal conductivity will tend to "even-out" the gradient in the flow direction. Heat will flow along the containment walls to the region where the heat transport in the fluid is most effective, that is in the inlet region. We have used a 3D finite element fluid code (CFD) for examining this effect, as well as the transition from a circular to a rectangular passage in the entrance to a stave. A study of the stave temperature versus length is not simple, but it is necessary if we are understand such issues as the heat path in the module attachment. It is this concern, that variants in adhesives, and adhesive bond line thickness can also have an appreciable affect that provides impetus to this study. To simplify this task, an all aluminum stave was constructed and tested with the single phase coolant, methanol-water, which is well understood.

The aluminum stave had a square channel cross-section with 3.2 mm dimension. We used the analytic expression given below to obtain the fluid film coefficient h(x).

$$Nu(x) = 3.66 + \frac{0.065\left(\frac{D_h}{x}\right)R_e P_r}{1 + 0.04\left[\left(\frac{D_h}{x}\right)R_e P_r\right]^{\frac{2}{3}}} \quad \text{and}$$

$$h(x) = \frac{Nu(x)K_t}{D_h}$$

One will notice that the relationships account for the hydraulic diameter(D_h), the Reynolds number(R_e) and Prandtl number(P_r), and the longitudinal coordinate x corresponding to the flow direction. A plot of the film coefficient obtained from these relationships is shown in Fig. 6. The very high coefficient (>4000W/(m^2-K)) corresponds to the entrance of the channel where the fluid is first initially comes in contact with the heated region. The film thermal gradient is very steep making heat transport into the fluid extremely effective. The solution that follows assumes a constant heat flux emanating from the pixel modules. This assumption differs from another classical solution for constant wall temperature in the longitudinal direction. As an observation, this high film coefficient near the entrance region causes heat to flow to this region in the stave body. We see this effect in our comparison with the experiment, Figs. 2-5. Each predicted point on these curves corresponds to a finite element thermal solution of the stave cross-section at that location. We modeled two different aluminum alloys and two adhesive layers in making this prediction. Notice that

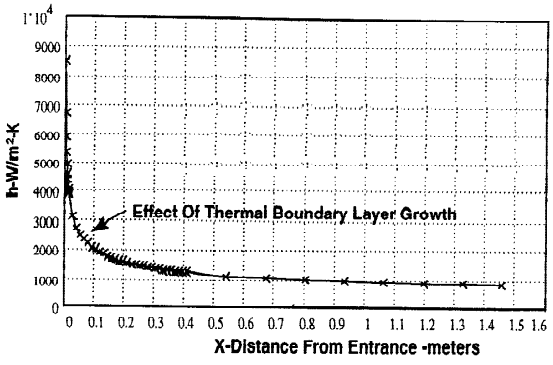

Fig. 6 Analytical calculation of the film coeeficient for 30% methanonl in water at -15°C.

the module surface temperature is slightly higher than would be predicted by our analysis. The difference is nominally 1.5 °C, out of 12 °C, or 12.5%, at the beginning of the channel. This is quite good considering all of the influences discussed above. The comparison with the experiment improves somewhat in the flow direction until we see a scatter developing in the data. We have reason to believe that the adhesive bond line that joined the last layer of aluminum (simulates the modules) was not bonded well. The adhesive used was DYMAX 991, a two part activator cured. This adhesive was replaced with a Masterbond adhesive and the scatter was reduced, but the overall drop was higher than anticipated, signifying that the bonding process had not been perfected. As cited, these tests were conducted with this specific purpose in mind, i.e., to understand the construction difficulties, as well as the behavior of the fluid.

With the FEA model we predicted the underneath temperature, i.e., on the stave underneath the side extensions that support the modules. Fig. 3 illustrates this comparison, which is somewhat improved. Similarly, the bottom of the cooling channel was predicted, this is shown in Fig. 4. This comparison for the most part is within 10%. Fig. 5 shows a comparison for reduced flow (lower Reynolds number). Again, the agreement is not bad.

V. BINARY ICE RESULTS

The prototype stave was transported to Rutherford Appleton Laboratory for measurements with binary ice, small ice crystals in a methanol-water mixture. The stave was mounted in a temperature controlled box and the ambient temperature was maintained at about - 0.3 °C. Measurements with methanol-water were repeated and agreed with data obtained at LBNL to within about 1°C, which can be attributed to the difference in ambient temperature. These measurements were done with the Masterbond adhesive.

The temperature distribution in the prototype was measured with binary ice with an ice

concentration of >2%. This number is inferred from the observation that not all of the ice had melted at the exit of the stave. The ice concentration was not easily controlled or measured during our measurements. The inlet temperature was about -12.7 °C. We have scaled the measurements to an inlet temperature of -15°C to compare to measurements with methanol-water at this temperature. The results are given in Fig. 7 for flow rates(the methanol-water flow rate was 12.8 cc/s and the binary ice flow rate was 13.7 cc/s) that yield pressure drops about 200 mbar. The binary ice is seen to provide a lower operating temperature and a more uniform temperature than methanol-water. The temperature of the "silicon" is everywhere less than -5°C, which is the temperature specification for the pixel system.

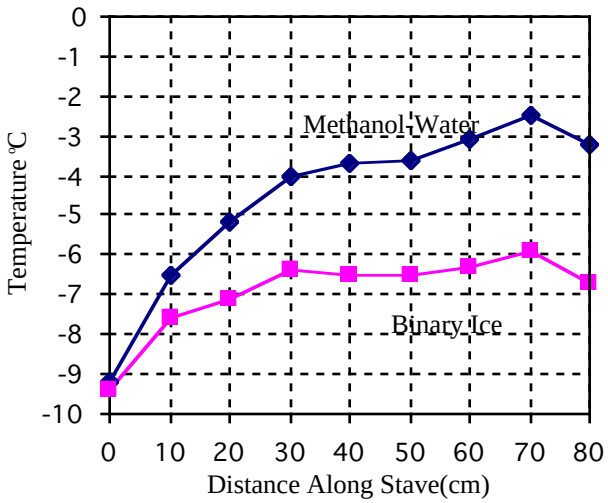

Fig. 7 Comparison of the "silicon" temperature of the prototype stave measured with 30% methanol in water and with binary ice under the conditions given in the text.

The temperature distribution for a higher flow rate was also measured and is compared with the lower flow rate in Fig. 8.

Our understanding of the binary-ice performance is based on the premise that the small ice crystals contained in the fluid greatly enhance the fluid specific heat capacity. We further reason that heat transport into the fluid is still dominated by conduction for the laminar flow condition in the stave channel. However,

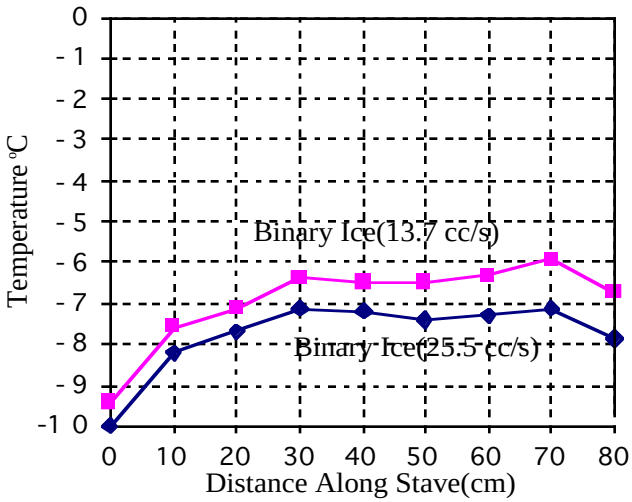

Fig. 8 Temperature distribution of the "silicon" on the prototype stave for different flow rates of binary ice.

now the heat need not be transported to the channel centerline to reach equilibrium, as long as the ice is not depleted, nor stratifies. Hence, one can anticipate a finite temperature difference will exist between the stave wall and the fluid, i.e., the wall temperature does not correspond to the fluid "bulk" temperature. We do indeed see a temperature difference in our results. Although the thermal entry length is shorter for the binary-ice fluid, its presence does exist, however. Isothermality of the aluminum stave structure was significantly improved by the binary-ice, over that of the single phase fluid. However, a length-wise variation on the order of 3 °C can be expected. Again, it was hoped by many that this temperature variation would be less.

There is much more to be learned about the binary-ice system performance. We expect that the extent to which we can achieve isothermality is primarily connected to ice concentration and mass flow rate. Fluid mixing, or turbulent flow would greatly enhance our options in this regard. However, these are not possible since we are constrained to maintain the pressure drop within the tracking volume to less than 200 mbar, thus we must seek an optimum set of flow parameters. We have just started to develop test experience with the binary-ice system that will lead to defining how the flow hydraulics and heat transport are related to ice-concentration.

VI. CONCLUSIONS

We have measured the temperature distribution in a prototype, full-length pixel stave operating with methanol-water and binary ice coolants. A combination of analytical and finite-element calculations of the temperature distribution using single-phase, methanol-water coolant are in good agreement with our measurements. This indicates that we have a good understanding of the thermal characteristics and can model future designs with some confidence. The binary ice methanol-water coolant provides a cooler and a more uniform temperature. The absolute temperature of the simulated silicon in the prototype meets the specification to maintain the pixel silicon detector temperature below -5^{o}C with binary ice coolant. Additional work is needed to characterize the binary ice coolant so that thermal modeling can be improved.

ACKNOWLEDGEMENTS

The measurements with binary ice were done at the Rutherford Appletion Laboratory and were made possible by R. Apsimon.